



# Manipulation of Dietary Amino Acids Prevents and Reverses Obesity in Mice Through Multiple Mechanisms That Modulate Energy Homeostasis

Chiara Ruocco,<sup>1</sup> Maurizio Ragni,<sup>1</sup> Fabio Rossi,<sup>1</sup> Pierluigi Carullo,<sup>2,3</sup> Veronica Ghini,<sup>4</sup> Fabiana Piscitelli,<sup>5</sup> Adele Cutignano,<sup>5</sup> Emiliano Manzo,<sup>5</sup> Rafael Maciel Ioris,<sup>6,7</sup> Franck Bontems,<sup>6,7</sup> Laura Tedesco,<sup>1</sup> Carolina M. Greco,<sup>2</sup> Annachiara Pino,<sup>8</sup> Ilenia Severi,<sup>9</sup> Dianxin Liu,<sup>10</sup> Ryan P. Ceddia,<sup>10</sup> Luisa Ponzoni,<sup>1,11</sup> Leonardo Tenori,<sup>12,13</sup> Lisa Rizzetto,<sup>14</sup> Matthias Scholz,<sup>14</sup> Kieran Tuohy,<sup>14</sup> Francesco Bifari,<sup>15</sup> Vincenzo Di Marzo,<sup>16,17</sup> Claudio Luchinat,<sup>4,18</sup> Michele O. Carruba,<sup>1</sup> Saverio Cinti,<sup>9</sup> Ilaria Decimo,<sup>8</sup> Gianluigi Condorelli,<sup>2,3,19</sup> Roberto Coppari,<sup>6,7</sup> Sheila Collins,<sup>10</sup> Alessandra Valerio,<sup>20</sup> and Enzo Nisoli<sup>1</sup>

*Diabetes* 2020;69:2324–2339 | <https://doi.org/10.2337/db20-0489>

**Reduced activation of energy metabolism increases adiposity in humans and other mammals. Thus, exploring dietary and molecular mechanisms able to improve energy metabolism is of paramount medical importance because such mechanisms can be leveraged as a therapy for obesity and related disorders. Here, we show that a designer protein-deprived diet enriched in free essential amino acids can 1) promote the brown fat thermogenic program and fatty acid oxidation, 2) stimulate uncoupling protein 1 (UCP1)-independent respiration in subcutaneous white fat, 3) change the gut microbiota composition, and 4) prevent and reverse obesity and dysregulated glucose homeostasis in multiple mouse models, prolonging the healthy life span. These effects**

**are independent of unbalanced amino acid ratio, energy consumption, and intestinal calorie absorption. A brown fat-specific activation of the mechanistic target of rapamycin complex 1 seems involved in the diet-induced beneficial effects, as also strengthened by in vitro experiments. Hence, our results suggest that brown and white fat may be targets of specific amino acids to control UCP1-dependent and -independent thermogenesis, thereby contributing to the improvement of metabolic health.**

Although debatable, chronic consumption of diets with a high ratio of saturated to unsaturated fatty acids (SFA

<sup>1</sup>Center for Study and Research on Obesity, Department of Biomedical Technology and Translational Medicine, University of Milan, Milan, Italy

<sup>2</sup>IRCCS Humanitas Clinical and Research Center, Rozzano, Italy

<sup>3</sup>Institute of Genetic and Biomedical Research, National Research Council, Rozzano, Italy

<sup>4</sup>Interuniversity Consortium for Magnetic Resonance, Sesto Fiorentino, Italy

<sup>5</sup>Institute of Biomolecular Chemistry, National Research Council, Pozzuoli, Italy

<sup>6</sup>Department of Cell Physiology and Metabolism, University of Geneva, Geneva, Switzerland

<sup>7</sup>Diabetes Center of the Faculty of Medicine, University of Geneva, Geneva, Switzerland

<sup>8</sup>Department of Diagnostics and Public Health, University of Verona, Verona, Italy

<sup>9</sup>Department of Experimental and Clinical Medicine, Marche Polytechnic University, Center of Obesity, Ancona, Italy

<sup>10</sup>Division of Cardiovascular Medicine, Department of Medicine, Vanderbilt University Medical Center, Nashville, TN

<sup>11</sup>Institute of Neuroscience, National Research Council, Milan, Italy

<sup>12</sup>FiorGen Foundation, Sesto Fiorentino, Italy

<sup>13</sup>Center of Magnetic Resonance, University of Florence, Sesto Fiorentino, Italy

<sup>14</sup>Department of Food Quality and Nutrition, Research and Innovation Center, Edmund Mach Foundation, San Michele all'Adige, Italy

<sup>15</sup>Laboratory of Cell Metabolism and Regenerative Medicine, Department of Medical Biotechnology and Translational Medicine, University of Milan, Milan, Italy

<sup>16</sup>Canada Excellence Research Chair Microbiome-Endocannabinoidome Axis in Metabolic Health, Université Laval, Quebec City, Canada

<sup>17</sup>Joint International Research Unit for Chemical and Biochemical Research on the Microbiome and Its Impact on Metabolic Health and Nutrition, Institute of Biomolecular Chemistry, National Research Council, Pozzuoli, Italy and Université Laval, Quebec City, Canada

<sup>18</sup>Department of Experimental and Clinical Medicine, University of Florence, Florence, Italy

<sup>19</sup>Humanitas University, Rozzano, Italy

<sup>20</sup>Department of Molecular and Translational Medicine, Brescia University, Brescia, Italy

Corresponding author: Enzo Nisoli, [enzo.nisoli@unimi.it](mailto:enzo.nisoli@unimi.it)

Received 8 May 2020 and accepted 6 August 2020

This article contains supplementary material online at <https://doi.org/10.2337/figshare.12771341>.

C.R. and M.R. contributed equally to this work.

© 2020 by the American Diabetes Association. Readers may use this article as long as the work is properly cited, the use is educational and not for profit, and the work is not altered. More information is available at <https://www.diabetesjournals.org/content/license>.

diets) increases body adiposity, impairs glucose homeostasis, raises the cardiovascular risk, and reduces the healthy disease-free life span in animals and humans (1,2). These diets negatively affect the proper secretion and action of key hormones—insulin, leptin, and adiponectin—underlying metabolic homeostasis and energy balance (3). The increased consumption of high-calorie, low-fiber diets has contributed significantly to the staggering rise in overweight, obesity, and type 2 diabetes prevalence in the past few decades (4). Likewise, high-protein diets have been advocated since the 1960s as a means of weight loss and to prevent obesity and its metabolic sequelae (5). However, the long-term safety of such diets has been recently questioned by increasing evidence of raised cardiovascular risk (6). Accordingly, great excitement was built by the demonstration that protein-restricted diets (7), or diets with lower concentrations of single or multiple essential amino acids (EAAs) (e.g., leucine, methionine, or tryptophan), were correlated to improved energy balance and decreased overweight or obesity in mice and humans (8,9). In contrast, several studies have also shown the efficacy of central or peripheral supplementation of a single amino acid (e.g., glycine, leucine, or tryptophan) in modulating energy metabolism and/or body weight (10,11). However, not all of these findings were confirmed by others (12).

To investigate these conflicting results, we conducted in-depth analyses on metabolic effects in normal-weight and obese mice caused by acute and chronic consumption of two customized diets. Specifically, the protein content (i.e., casein) of the SFA diet (10% fat) and high-fat diet (HFD, 60% fat) was substituted with an original formula composed by EAAs (SFA-EAA and HFD-EAA) (for nutrient compositions see below). The EAA mixture was stoichiometrically similar to the formula we previously showed to promote mitochondrial biogenesis in skeletal and cardiac muscles of middle-aged mice and to ameliorate health, especially in older adult mice, when consumed as a dietary supplement with drinking water (13,14). The metabolic effects of SFA-EAA and HFD-EAA diets were compared with those owed to two isocaloric, isolipidic, and isonitrogenous diets, identical to the SFA diet or HFD except for casein replacement by the purified amino acid mixture designed on the amino acid profile of casein (SFA-CAA and HFD-CAA diets), in addition to those induced by a chow diet. In particular, drinking supplementation of the EAA mixture was found to prevent oxidative stress in metabolically active cells (14–16), ameliorating muscle and cognitive performance in diverse animal models and humans (17,18). Moreover, a relevant rejuvenation was observed in the gut microbiota of aging mice supplemented with the EAA mixture (19). This observation seems to be of relevance, because diet composition may affect energy balance also through intestinal microbiota. For example, dietary amino acid intake increases the relative abundance of *Bacteroidetes* (20), and EAA-derived short-chain fatty acids modulate the overall lipid balance and glucose metabolism (21). Also, the gut

microbiota controls adiposity (22) and can activate adaptive thermogenesis in mice (23).

Adaptive thermogenesis refers to the generation of heat by the body in response to external stimuli (e.g., cold temperature, ingestion of high-calorie foods). It includes shivering and nonshivering thermogenesis (NST). The activation of brown adipocytes in brown adipose tissue (BAT) and beige adipocytes in visceral and subcutaneous fat depots contributes substantially to NST (24). These thermogenic adipocytes express uncoupling protein 1 (UCP1), a protein that uncouples respiration and leads to energy dissipation in the form of heat. Ablation of brown or beige adipocytes predisposes mice to develop obesity and type 2 diabetes (25,26), as does deletion of the *Ucp1* gene (27). Conversely, increasing the number or activity of thermogenic adipocytes protects against body weight gain and metabolic disease (28). Activation of mechanistic target of rapamycin complex 1 (mTORC1) is required for BAT recruitment and metabolic adaptation to cold (29,30). Additional mechanisms activate thermogenesis in an UCP1-independent manner: the glycerol phosphate shuttle, calcium-dependent ATP hydrolysis, and creatine-dependent substrate cycling (31–33). Also, *N*-acyl amino acids stimulate uncoupled mitochondrial respiration in white adipocytes, independently of UCP1, and their systemic administration activates the whole-body energy expenditure (34).

Here we show that almost complete substitution of the casein in standard rodent diets with a unique amino acid mixture modulated energy homeostasis in diet-induced obesity or a model of genetic obesity. Our results reveal multiple thermogenic mechanisms by which designer diets could be used to combat obesity and type 2 diabetes.

## RESEARCH DESIGN AND METHODS

### Animals, Diets, and Treatments

Male C57BL/6N mice (8 weeks old), from Charles River (Calco, Italy), were weight-matched and fed ad libitum for different periods of time with a normal chow diet (V1534-300; Ssniff Spezialdiäten GmbH, Soest, Germany), SFA diet (20% protein, namely casein, 70% carbohydrate, and 10% fat, half of which was lard [D12450H]), HFD (20% protein, 10% carbohydrate, and 60% fat [D12492]), or two isocaloric, isolipidic, and isonitrogenous diets identical to the SFA diet or HFD except for protein, which was almost completely (93.5%) replaced by defined free EAAs (SFA-EAA [D14032501] or HFD-EAA [D17073104]) or a purified amino acid mixture designed on the amino acid profile of casein (SFA-CAA diet [A17092801] or HFD-CAA [A20040601]), all from Research Diets (Brogaarden, Gentofte, Denmark) (Supplementary Table 1).

Body weight and food intake were recorded twice a week in mice housed individually (except for the survival study). A cohort of C57BL/6N (8 weeks old) and *ob/ob* (6 weeks old, C57BL/6J background) male mice were kept and examined at thermoneutrality (30°C) for the entire

treatment period. For norepinephrine (NE) turnover analysis, mice fed for 6 weeks with SFA-CAA and SFA-EAA diets were i.p. treated with  $\alpha$ -methyl-*para*-tyrosine (Sigma-Aldrich) at time 0 (300 mg/kg body wt) and after 2 h (150 mg/kg body wt). Mice were sacrificed after 4 h, and NE content was determined on interscapular BAT (iBAT) with the Noradrenaline High Sensitive ELISA kit (Diagnostika GmbH, Hamburg, Germany), following the manufacturer's instructions. For selective inhibition of mTORC1, mice were i.p. injected with rapamycin (2.5 mg/kg body wt) or vehicle (0.2% carboxymethylcellulose, 0.25% Tween 80 in sterile water) (all from Sigma-Aldrich), 5 days per week for 6 weeks, starting with diets. All mice used have a C57BL/6N background that does not exhibit defects of insulin release and mitochondrial dysfunction relative to C57BL/6J mice (35). Body composition was determined using the EchoMRI-100 system (Houston, TX), as previously described (36). Tissue samples for molecular analysis were snap frozen in liquid nitrogen and prepared as described below. All animal procedures were conducted in accordance with the European Community Guidelines and those of the Italian Ministry of Health and complied with the National Animal Protection Guidelines.

#### Caloric Absorption and Gut Motility

At the end of the treatments, feces were collected from each mouse, and energy content was measured by calorimetric bomb analysis (AC-350; LECO, Milan, Italy). To monitor gut motility, whole-gut transit time was measured as described (37). As parameters of absorbent capacity and epithelial morphology, the villi length of jejunum from frozen sections of intestine was determined by the Nikon Lucia IMAGE (v. 4.61) image analysis software (37).

#### Glucose Homeostasis and Biochemical Analysis

Glucose and pyruvate tolerance tests were performed after overnight fasting by i.p. injection of glucose or pyruvic acid (each 1.5 g/kg body wt) (Sigma-Aldrich). An insulin tolerance test was performed after a 4-h daytime fast, with 0.5 units/kg body wt insulin i.p. injection (Sigma-Aldrich). Glucose levels were measured in tail vein blood using a Glucometer MyStar Extra (Sanofi, Milan, Italy) and test strips at different times after the bolus. Plasma biochemistry and thyroxine levels were provided by Charles River Laboratories Service (Charles River Clinical Pathology/Immunology Laboratories, Wilmington, MA). Metabolites and hormones were measured by commercial kits (Supplementary Table 2). Mean lipid droplet density and area in iBAT were measured by the Nikon Lucia IMAGE (v. 4.61) image analysis software and calculated in 25 brown adipocytes for each sample.

#### Behavioral Tests

The social dominance tube test and the elevated plus-maze test were performed with mice fed with the SFA, SFA-CAA,

and SFA-EAA diets for 20 months, as described (38). Spontaneous motor activity was evaluated using an activity cage (Ugo Basile, Varese, Italy) placed in a sound-attenuating room, and an object recognition test was conducted in an open plastic arena.

#### Indirect Calorimetry, Locomotor Activity, and Temperature Measurements

Metabolic efficiency was calculated as the ratio between body weight gain and the total energy intake over 5 days or 2 or 6 weeks. For in vivo indirect calorimetry analysis, mice were transferred to a Phenomaster System (TSE Systems GmbH, Bad Homburg, Germany) 1 week before the study started for acclimatization, followed by 3 weeks of continued measurements, as previously described (36). Core body temperature was obtained with a rectal probe (Physitemp Instruments, Clifton, NJ). To estimate the level of iBAT thermogenesis, shaved back temperature was measured by infrared thermography with a thermoelectrically cooled ThermoCAM P25 (FLIR Systems, Wilsonville, OR) (37). In vivo images were captured and analyzed using the FLIR QuickReport software according to the manufacturer's specifications.

#### Mass Spectrometry Analysis

Plasma samples and iBAT were extracted from mice after night feeding, and their amino acid content was quantitated using the AccQ-Tag derivatization reagent provided by Waters Chromatography Europe BV (Etten-Leur, the Netherlands). All amino acids were acquired in positive polarity, in both time-of-flight mass spectrometry and product ion mode, according to the  $m/z$  values reported in Supplementary Table 3.

#### Fecal Microbiota Analysis

Fresh feces were collected, immediately frozen, and stored. After extraction of total DNA (FastDNA SPIN Kit for Feces, MP Biomedicals), 16S rRNA sequencing analysis was performed. Quantitative Insights into Microbial Ecology (QIIME) was used to determine  $\alpha$ - and  $\beta$ -diversity. Data are accessible at the European Nucleotide Archive with the accession number PRJEB25686.

#### Primary Brown Adipocytes

Mouse brown fat precursor cells were enzymatically isolated from iBAT of C57BL/6N male mice and differentiated in culture for 9 days as previously described (39). Primary brown adipocytes maintained in amino acid-free DMEM (USBiological Life Science, DBA, Milan, Italy) for 16 h, were pretreated with rapamycin (1.0 nmol/L) or vehicle (DMSO; Sigma-Aldrich) for 1 h and subsequently supplemented for a further 24 h with one of two different amino acid combinations, precisely reproducing the iBAT aminograms resulting from consumption of the SFA-CAA or SFA-EAA diet (Supplementary Table 4). Cellular oxygen consumption rates (OCRs) were determined using a Seahorse XF24 Extracellular Flux Analyzer (Agilent, Santa Clara, CA).

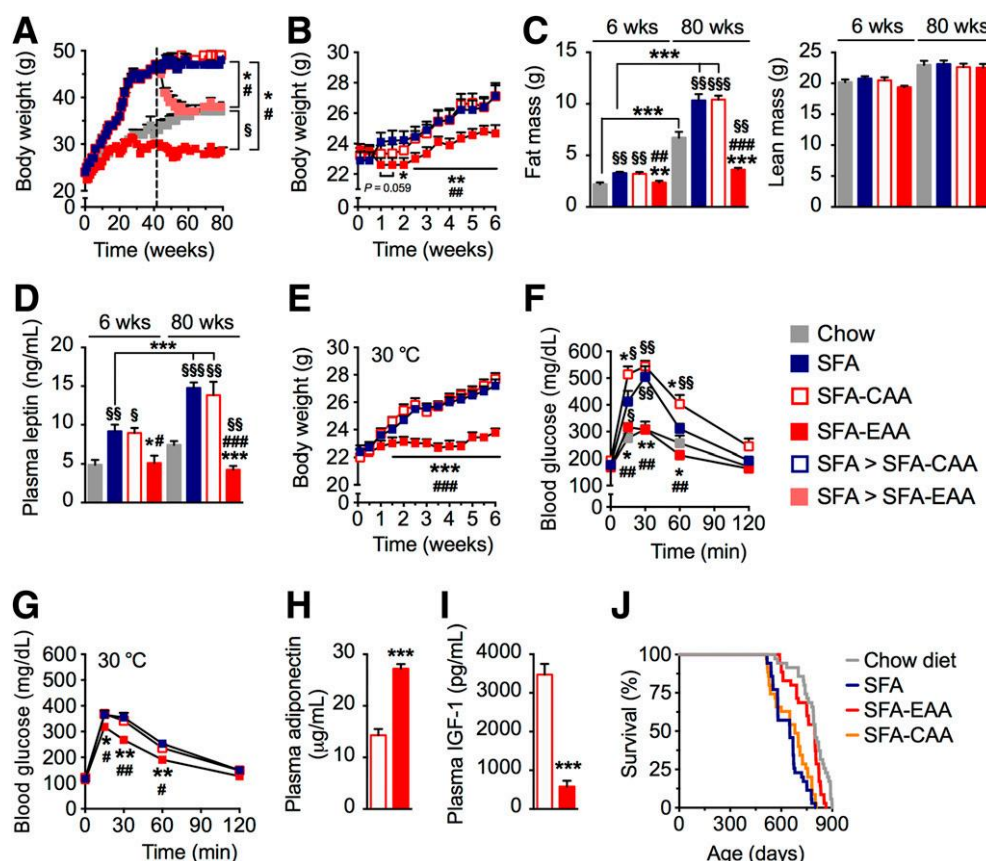


**Figure 1**—EAA, unlike CAA substitution for protein content of rodent diets, prevents and reverses obesity, with the improvement of glucose homeostasis and extension of average life span. **A:** Body weight of mice fed with the chow, SFA, SFA-EAA, and SFA-CAA diet at room temperature ( $n = 7$ – $10$  mice per group). After maximal body weight was reached (11 months, dashed line), mice fed with the SFA diet were switched to either the SFA-EAA diet (SFA to SFA-EAA) or the SFA-CAA diet (SFA to SFA-CAA) ( $n = 5$  mice per group). **B:** Body weight of mice at room temperature ( $n = 9$ – $10$  mice per group). **C:** Body composition at the end of treatment: fat mass (left) and lean mass (right) ( $n = 6$  mice per group). **D:** Plasma leptin levels at different times at room temperature ( $n = 5$  mice per group). **E:** Body weight of mice at thermoneutrality ( $30^{\circ}\text{C}$ ) ( $n = 10$  mice per group). Glucose tolerance test results in mice at room temperature ( $n = 5$  mice per group) (**F**) or at thermoneutrality (**G**) ( $n = 7$  mice per group). Mice were fed with different diets for 6 weeks. Plasma levels of adiponectin (**H**) and IGF-1 (**I**) in mice fed with the SFA-CAA or SFA-EAA diet for 6 weeks at room temperature ( $n = 5$  mice per group). **J:** Kaplan-Meier survival curves for chow, SFA-, SFA-EAA-, and SFA-CAA-fed mice ( $n = 35$  mice per group). All data (except **J**) are presented as mean  $\pm$  SEM. \* $P < 0.05$ , \*\* $P < 0.01$ , and \*\*\* $P < 0.001$  vs. SFA diet; # $P < 0.05$ , ## $P < 0.01$ , and ### $P < 0.001$  vs. SFA-CAA diet; § $P < 0.05$ , §§ $P < 0.01$ , and §§§ $P < 0.001$  vs. chow diet.

Before analysis, the culture medium was changed to respiration medium. After basal respiration, uncoupled and maximal respiration was determined after the addition of oligomycin ( $1 \mu\text{mol/L}$ ) and subsequently carbonyl cyanide 4-(trifluoromethoxy)phenylhydrazone (FCCP,  $0.2 \mu\text{mol/L}$ ). Rotenone ( $3 \mu\text{mol/L}$ ) was used to abolish mitochondrial respiration. All reagents were purchased from Sigma-Aldrich.

### Gene Expression and Mitochondrial Physiology

Quantitative RT-PCR reactions were performed as described (32) and run with the iQ SYBR Green I SuperMix (Bio-Rad, Segrate, Italy) on an iCycler iQ Real-Time PCR detection system (Bio-Rad). mtDNA was amplified using primers specific for the mitochondrial cytochrome b gene and normalized to genomic DNA (gDNA). Primers were designed using Primer3 (v. 0.4.0) software and are shown in Supplementary Table 5. Immunoblot analysis was

performed as described (32). The antibodies (each at 1:1,000 dilution) are reported in Supplementary Table 6. Citrate synthase activity was measured spectrophotometrically in gastrocnemius, as previously described (32). Carnitine palmitoyltransferase I (CPT1) activity was measured spectrophotometrically in iBAT mitochondria, as previously described (40). Electron microscopy analysis was conducted in thin sections of iBAT stained with lead citrate and examined with a CM10 transmission electron microscope (Philips, Eindhoven, the Netherlands). Mitochondrial OCR was measured in a gas-tight vessel equipped with a Clark-type oxygen electrode (Rank Brothers Ltd., Cambridge, U.K.). Briefly, mitochondria from inguinal white adipose tissue (iWAT) and iBAT were isolated, and respiration was measured as described (34). Liver and gastrocnemius mitochondria respiration was assessed in  $137 \text{ mmol/L KCl}$ ,  $10 \text{ mmol/L HEPES}$  (pH 7.2),  $2.5 \text{ mmol/L MgCl}_2$ ,  $0.1\% \text{ BSA}$ , and  $2 \text{ mmol/L}$

$K_2HPO_4$ . iBAT OCR was measured by sequential addition of 2.5 mmol/L malate, 30  $\mu$ mol/L palmitoyl-CoA plus 5 mmol/L carnitine, 2 mmol/L guanosine-5'-diphosphate (GDP), 100  $\mu$ mol/L ADP, 0.01 mg/mL oligomycin, and FCCP (500 nmol/L), all from Sigma-Aldrich. UCP1-dependent respiration was calculated as the amount of ADP-independent respiration that was inhibited by GDP, as previously described (24). For iWAT, liver, and gastrocnemius, the same substrates, except GDP, were used.

#### **N-Acyl Amino Acid and Acylcarnitine Measurements by Liquid Chromatography-High Resolution Mass Spectrometry**

N-Acyl amino acids were synthesized and measured, as previously described (34). Targeted quantitative analysis was performed on extracted ion chromatograms corresponding to the molecular ion  $m/z$  values  $[M-H]^-$  for N-acyl amino acid and  $[M+H]^+$  for long-chain acylcarnitines. Quantitation of N-acyl amino acid and long-chain acylcarnitines was performed by integrating the area under the peak of each natural compound and normalizing to the corresponding internal standard area value.

#### **Statistical Analyses**

Statistical analysis was performed by unpaired Student  $t$  test for two-group analysis or one-way ANOVA with Tukey correction or two-way ANOVA with Bonferroni correction for multiple group comparisons. Kaplan-Meier survival curves were created with the log-rank test equal to the Mantel-Haenszel test. A  $P$  value  $<0.05$  was considered statistically significant. Correlations were determined by the nonparametric Spearman correlation test using the computer program GraphPad Prism (v. 6.04).

#### **Data and Resource Availability**

The data sets generated and analyzed during the current study are available from the corresponding author upon reasonable request.

## **RESULTS**

#### **Effects on Body Weight, Body Composition, and Adipose Tissue**

The subacute (6-week) and chronic (80-week) consumption of the SFA diet increased body weight and adiposity independently of body length and lean mass, with higher circulating leptin levels compared with mice fed the chow diet (Fig. 1A–D and Supplementary Fig. 1A). Feeding mice with the SFA-EAA diet prevented obesity development, maintaining lower fat mass and circulating leptin levels, without affecting lean mass or the normal growth of mice (Fig. 1A–D and Supplementary Fig. 1A and B). Notably, after 44 weeks, mice fed with the SFA-EAA diet weighed less than mice fed with the chow diet, with reduced body weight and adiposity until sacrifice (Fig. 1A and C). In addition to this preventive antiobesity action, our designer diet exerted a potent therapeutic effect in which mouse body weight dropped after the switch from the SFA diet to

the SFA-EAA diet (Fig. 1A). Body weight of the SFA-fed mice that were switched to the SFA-EAA diet indeed decreased to the level of the chow-fed mice in  $\sim 2.5$  months (Fig. 1A). Notably, the specific EAA substitution for casein entirely prevented the body weight gain, fat mass accumulation, and adiposity also induced by HFD consumption (Supplementary Fig. 2A–C). Similarly, the HFD-EAA diet strongly reduced body weight in already obese mice (Supplementary Fig. 2A, left). By contrast, both CAA-substituted diets were unable to prevent the obesity development or reduce body weight in already obese animals (Fig. 1A–D and Supplementary Fig. 2A–C).

The experiments mentioned above were conducted at room temperature (i.e., at  $\sim 22^\circ\text{C}$ ), a condition known to cause an increase of food intake and metabolism in small rodents to maintain body temperature (41). Thus, to determine the contribution of environmental thermal stress, we tested the metabolic effect of our engineered diets in C57BL6/N and leptin-deficient *ob/ob* mice at thermoneutrality (41). Our additional experiments confirmed the healthy effects of the SFA-EAA diet under this condition (Supplementary Fig. 2D).

#### **Effects on Glucose Homeostasis and Adipokines**

Mice fed with the SFA-EAA diet for either 6 weeks or 11 months at room temperature had improved glucose and pyruvate tolerance and insulin-induced glycemia-lowering response compared with those of mice fed with either the SFA or SFA-CAA diets (Fig. 1F and Supplementary Fig. 1C–G). Fasting blood glucose and insulin concentrations did not differ among mice fed with different diets (Supplementary Table 2). These phenotypes were also observed when the SFA-EAA diet was consumed at  $30^\circ\text{C}$  in C57BL6/N (Fig. 1G) and *ob/ob* mice (Supplementary Fig. 2E), and in HFD-EAA-fed mice at room temperature (Supplementary Fig. 2F and G). These results were confirmed by the circulating levels of adiponectin ( $89 \pm 15\%$  higher,  $P < 0.05$ ) in mice fed with the SFA-EAA diet compared with mice fed with the SFA-CAA diet (Fig. 1H). Accordingly to its inverse association to adiponectin in type 2 diabetes (42), IGF-I was reduced in the plasma of SFA-EAA-fed mice compared with SFA-CAA-fed animals (Fig. 1I).

#### **Effects on the Whole-Body and Hepatic Lipid Metabolism**

Management of dyslipidemia is a crucial approach to reduce cardiovascular risk in patients with obesity or diabetes. Plasma nonesterified fatty acid (NEFA) levels, higher after consumption of the obesogenic diets (SFA and HFD), were reduced in both SFA-EAA- and HFD-EAA-fed mice to values observed in mice fed the chow diet (Supplementary Fig. 3A). Total cholesterol plasma levels were increased in HFD-fed mice, whereas circulating triglycerides were similar between groups (Supplementary Fig. 3B and C). Unlike the HFD-CAA diet, the HFD-EAA diet statistically prevented cholesterol increase induced by the HFD (Supplementary Fig. 3B). These systemic effects



were mirrored by the ability of the SFA-EAA and HFD-EAA diets to both prevent the increased NEFA, triglyceride, and cholesterol levels of the liver in SFA- and HFD-fed mice (Supplementary Fig. 3D–F). Accordingly, macroscopic liver appearance and liver weight confirmed these results (Supplementary Fig. 3G and H). Mitochondrial respiration with palmitoyl carnitine as the substrate suggested that EAA substitution promoted fat oxidation in the liver of both SFA- and HFD-fed mice (Supplementary Fig. 3I). Both CAA-substituted diets were ineffective.

### Plasma Amino Acids

We next evaluated the effects of diets on amino acids in plasma. Alanine, glutamine, lysine, and threonine were higher with both the EAA- and CAA-substituted diets than with the SFA diet, although threonine was much more increased in SFA-EAA- than SFA-CAA-fed mice (Supplementary Fig. 4). In addition to threonine, the SFA-EAA diet increased histidine and valine levels over both the SFA and SFA-CAA diets (Supplementary Fig. 4). Glycine and serine levels, which were markedly augmented in the SFA-CAA mice, were similar with the SFA-EAA diet to those observed in the SFA-fed mice (Supplementary Fig. 4). Notably, the levels of valine, histidine, and threonine were inversely correlated to the body weight and adiposity, isoleucine was inversely correlated to the body weight but not adiposity, while leucine was correlated with neither (Supplementary Table 7). Moreover, tyrosine was positively correlated to fat accumulation, while an inverse correlation was observed between plasma levels of histidine and the liver weight and liver mitochondrial respiration (Supplementary Table 7). Of note, under our experimental conditions, no statistical correlation was observed with insulin sensitivity. SFA-EAA consumption did not affect liver and kidney function parameters (Supplementary Table 2).

### SFA-EAA Diet Extends Healthy Life Span

Next, we investigated the effects of the SFA-EAA diet on mouse life span. The median life span for mice fed the chow diet was 800 days. Life span was extended from 650 days for SFA mice and 680 days for SFA-CAA mice to 797 days for SFA-EAA mice (+23% vs. SFA and +17% vs. SFA-CAA) (Fig. 1J). Maximal life span was 899 days for chow-fed, 800 days for SFA-fed, 806 days for SFA-CAA-fed, and 863 days for SFA-EAA-fed mice. While mice fed with the SFA and SFA-CAA diets exhibited submissive/lethargic behavior after 20 months, mice fed with the SFA-EAA diet preserved energetic behavior. This was demonstrated by a test for social dominance, with a positive trend toward less fearful behavior measured in the elevated plus-maze and in spontaneous motor activity (Supplementary Fig. 5A–C). There was no apparent difference in the novel object recognition memory test among dietary groups (Supplementary Fig. 5D).

### Effects on Food Intake and Energy Absorption

We then assessed energy input and output. Because our mice drank only water and thus did not consume any

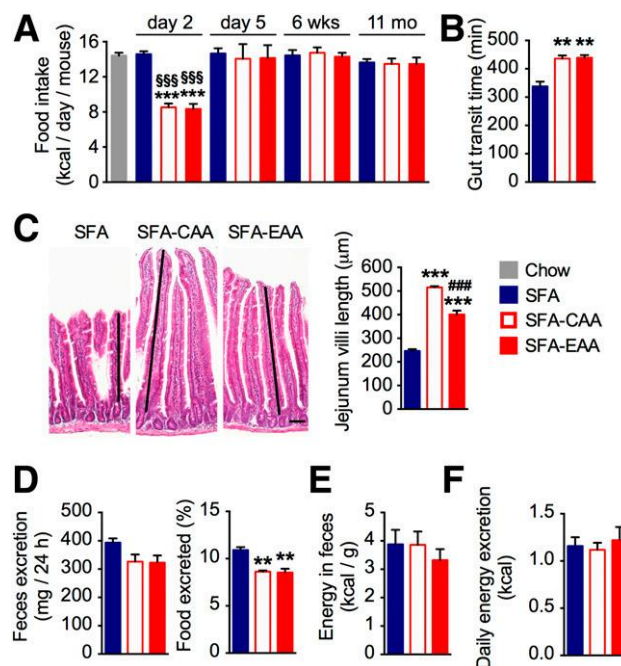


**Figure 2**—Food intake and energy absorption in mice on different dietary regimens. **A:** Food intake of mice fed with chow, SFA, SFA-EAA, and SFA-CAA diets for different time intervals ( $n = 5-7$  mice per group). **B:** Gut transit time. **C:** Hematoxylin and eosin staining of jejunum villi. Scale bar, 90  $\mu\text{m}$ . **D:** Energy excretion: the mean amount of feces excreted per mouse in 24 h (mg/24 h) (left) and food excreted (dry mass of fecal pellets, collected over 72 h and expressed as the percentage of food intake) (right). **E:** Mean energy content in feces (kcal/g). **F:** Daily energy excretion (kcal/mouse) calculated using the previous values ( $n = 3-5$  mice per group). **B–F:** Mice were fed with the SFA, SFA-CAA, and SFA-EAA diets for 6 weeks. All data are presented as mean  $\pm$  SEM. \*\* $P < 0.01$  and \*\*\* $P < 0.001$  vs. SFA diet; ### $P < 0.001$  vs. SFA-CAA; \$\$\$ $P < 0.001$  vs. chow diet.

calories through drinking, energy input was measured as food intake and energy absorption. During the first 2 or 5 days of the dietary challenge, mice fed with the EAA-substituted diets decreased their food intake compared with the respective controls; nevertheless, these differences vanished at later time points (Fig. 2A and Supplementary Fig. 6A–C). Similarly, the SFA-CAA- and HFD-CAA-fed mice decreased their food intake during the 1st days (Fig. 2A and Supplementary Fig. 6A). Because these mice gained a comparable amount of body weight as the SFA- and HFD-fed mice (Fig. 1B and Supplementary Fig. 3A), the SFA-CAA- and HFD-CAA-fed mice served as pair-fed control to SFA-EAA- or HFD-EAA-fed mice, respectively; henceforward, the SFA-CAA and HFD-CAA diets were considered the proper control diets.

Given changes in the ratio of EAAs and nonessential amino acids (NEAAs) in both SFA-EAA and HFD-EAA versus casein- or CAA-containing diets, we investigated whether some of the results obtained with the SFA-EAA and HFD-EAA diets are mediated by the detection of a perturbed amino acid balance by the liver or brain. We studied the activity of the critical regulator of cellular

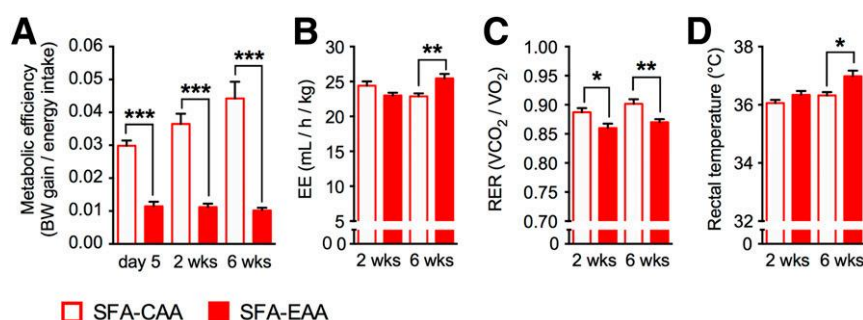


**Figure 3**—Energy metabolism in mice on different dietary regimens. A: Metabolic efficiency was calculated as the body weight (BW) gain-to-the energy intake ratio (i.e., total food consumed during 5 days or 2 or 6 weeks). EE (B) and RER (C) during one 24-h cycle. D: Whole-body temperature measured with a digital rectal thermometer. Measurements were performed in two separate experiments after 2 or 6 weeks ( $n = 5$ –7 mice per group). All data are presented as mean  $\pm$  SEM. \* $P < 0.05$ , \*\* $P < 0.01$ , and \*\*\* $P < 0.001$  vs. SFA-CAA diet.

responses under amino acid deficiency sensor, the kinase general control nonderepressible 2 kinase (GCN2). When activated by accumulation of uncharged tRNAs, GCN2 phosphorylates the  $\alpha$ -subunit of eukaryotic translation initiation factor 2 (eIF2), inhibiting general protein synthesis and mitigating the cellular stress (43). We found that the SFA-EAA diet did not change the Ser51-phosphorylation of eIF2 $\alpha$  in both the hypothalamus and liver compared with the SFA and SFA-CAA diets (Supplementary Fig. 6D), suggesting that the effects of the EAA-substituted diets are unlikely caused by detection of a dietary amino acid unbalance.

Next, we assessed the gut size and absorptive capacity of the different dietary regimens. SFA-EAA- and SFA-CAA-fed mice both had increased transit time and jejunum villi length compared with SFA-fed animals (Fig. 2B and C). Their percentage of food mass excretion was lower compared with SFA-fed mice, with only a trend to a decreased amount of feces excretion (Fig. 2D), suggesting that both substituted diets may cause malabsorption, albeit they affect differently body weight. Thus, we investigated whether the SFA-EAA and SFA-CAA exposure led to changes in calorie uptake by measuring the fecal caloric content with bomb calorimetry. This analysis revealed a comparable energy content in the fecal material of mice fed with the SFA-EAA or SFA-CAA diet (Fig. 2E), resulting in similar daily energy excretion in both groups compared with SFA-fed mice (Fig. 2F), also when expressed as a percentage of the food intake. These data indicate that food malabsorption is unlikely to be the underlying cause of the SFA-EAA diet's antiobesity action.

#### Effects on Energy Expenditure and Physical Activity

We next sought to understand whether energy expenditure was responsible for the observed phenotypes in mice fed with the different diets. Metabolic efficiency decreased in the SFA-EAA- and HFD-EAA-fed mice compared with the SFA-CAA- and HFD-CAA-fed animals, respectively, starting at day 5 of treatment (Fig. 3A and Supplementary Fig. 7A), suggesting that the EAA-designer diets may target energy homeostasis to reverse the obesity-disturbed metabolism favorably. VO<sub>2</sub> and energy expenditure (EE) were

measured in the different dietary groups (Supplementary Table 8). Of note, although no difference was observed in mice treated for 2 weeks, VO<sub>2</sub> and EE were higher in mice fed with the EAA-substituted diets for 6 weeks (Fig. 3B, Supplementary Fig. 7B, and Supplementary Table 8). Locomotor activity, which is a contributor to total energy expenditure, was normal in mice fed with all of the substituted diets (Supplementary Table 8). The respiratory exchange ratio (RER) was reduced in SFA-EAA- and HFD-EAA-fed mice compared with SFA-CAA- and HFD-CAA-fed mice at both time treatments (Fig. 3C and Supplementary Fig. 7C). This result is consistent with preferential oxidation of lipid fuels in SFA-EAA and HFD-EAA mice. Moreover, the increase of core body temperature was evident only after 6 weeks of SFA-EAA feeding (Fig. 3D) and was independent of circulating levels of the thyroid hormones thyroxine (total T4) and thyroid-stimulating hormone (Supplementary Table 2). Similar results were also observed in HFD-EAA compared with HFD-CAA mice (data not shown).

#### Effects on Gut Microbiota

No significant difference in microbial richness between diets was evident with three different  $\alpha$ -diversity estimators (Fig. 4A). The unsupervised multivariate statistical analysis—based on Bray-Curtis dissimilarity distance (principal coordinate analysis)—showed that the gut microbiota of the SFA-EAA group represented a structural shift mainly along with the second principal component (Fig. 4B). In contrast, the gut microbiota of the SFA and SFA-CAA groups were not separated (Fig. 4B). Moreover, the Bray-Curtis dissimilarity index between the SFA and SFA-EAA groups was significantly higher compared with each within-group dissimilarity and compared with that between the SFA and SFA-CAA groups (false discovery rate [FDR]  $P < 0.001$ ) (Fig. 4C). Despite taxon-based analysis revealing small effects, consumption of the SFA-EAA diet promoted an enrichment of *Allobaculum* and *Sutterella* relative abundance compared with the SFA (FDR  $P = 0.029$ ) and SFA-CAA (FDR  $P = 0.032$ ) diets; in turn, the SFA diet enriched *Lactococcus* compared with the SFA-CAA diet (FDR  $P = 0.029$ ) (Fig. 4D and E and

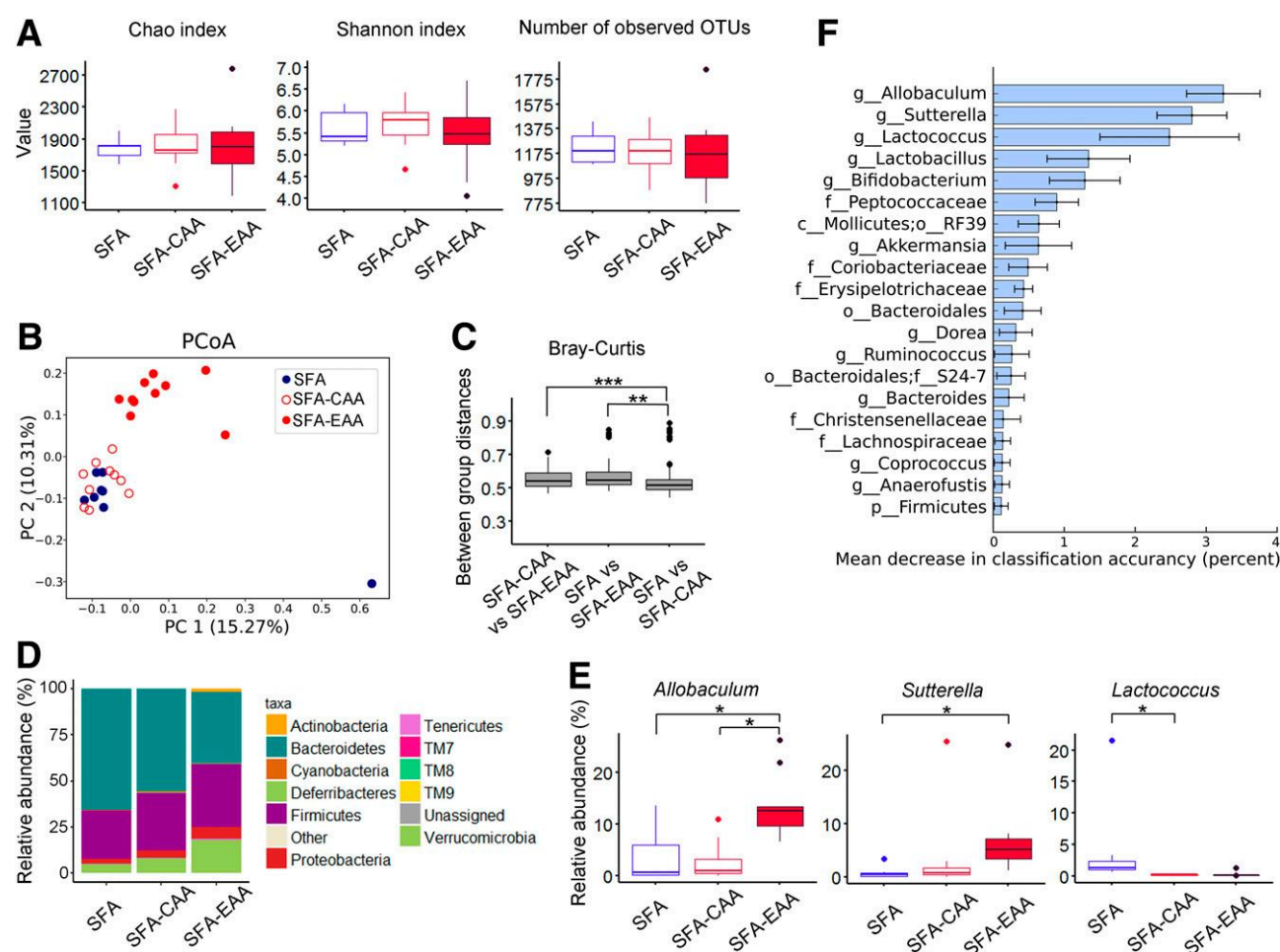


**Figure 4**—SFA-EAA diet changes gut microbiota composition. **A**: Chao index, Shannon entropy index, and  $\alpha$ -diversity calculated on the number of observed operational taxonomic units (OTUs). **B**: Principal coordinates analysis (PCoA) of bacterial  $\beta$ -diversity based on the Bray-Curtis dissimilarity index. Each symbol represents a single sample of feces after 6 weeks of treatment. **C**: Box-and-whisker plot of intercommunity  $\beta$ -diversity determined by the Bray-Curtis dissimilarity index. **D**: Phylum/order level relative abundance expressed as geometric mean. **E**: *Allobaculum*, *Sutterella*, and *Lactococcus* relative abundance. **F**: Random forest analysis. For the box-and-whisker plots, the boxes show median and first and third quartiles. The whiskers extend from the quartiles to the last data point within 1.5 $\times$  interquartile range, with outliers beyond represented as dots ( $n = 10$  mice per group). \* $P < 0.05$ , \*\* $P < 0.01$ , and \*\*\* $P < 0.001$  as shown.

Supplementary Table 9). Furthermore, *Allobaculum*, *Sutterella*, and *Lactococcus* were shown as the most discriminant bacterial taxa between SFA- and SFA-EAA-fed mice by random forest analysis (Fig. 4F). Notably, *Allobaculum* relative abundance inversely correlated with the body weight (Spearman  $r = -0.381$ ,  $P < 0.05$ ), insulin tolerance (Spearman  $r = -0.529$ ,  $P < 0.005$ ), and glucose metabolism (Spearman  $r = -0.704$ ,  $P < 0.01$ ). Similarly, *Sutterella* inversely correlated with insulin tolerance (Spearman  $r = -0.671$ ,  $P < 0.01$ ) and glucose metabolism (Spearman  $r = -0.532$ ,  $P < 0.05$ ) as well as *Akkermansia* with a reduced body weight (Spearman  $r = -0.613$ ,  $P < 0.05$ ).

#### Effects on Thermogenic White Adipocytes

To assess the role of adaptive thermogenesis in the action of the SFA-EAA diet, we investigated whether the EAA-substituted diets were able to promote the differentiation of beige adipocytes within iWAT. Gene expression profiling

after treatment did not find a statistical increase of markers of beige adipocytes in iWAT as well as of the thermogenic genes *Ucp1* and PR domain containing 16 (*Prdm16*), the positive inducer of mitochondrial biogenesis endothelial nitric oxide synthase (*eNOS*) (39), or the mitochondrial biogenesis markers in mice fed with the SFA-EAA diet (Supplementary Fig. 8A–C). Moreover, the expression of genes involved in lipolysis and fatty acid oxidation remained unchanged, while NEFA levels were decreased in iWAT of SFA-EAA-fed mice compared with controls (Supplementary Fig. 8D). The histological analysis confirmed these results, suggesting that browning is unlikely to play an important role in the metabolic actions of the SFA-EAA diet (Supplementary Fig. 8E).

By contrast, we found that uncoupled respiration was higher in iWAT mitochondria of wild-type or *ob/ob* mice fed with the SFA-EAA diet than with the SFA-CAA diet at 30°C, a condition in which there is no expression of UCP1.



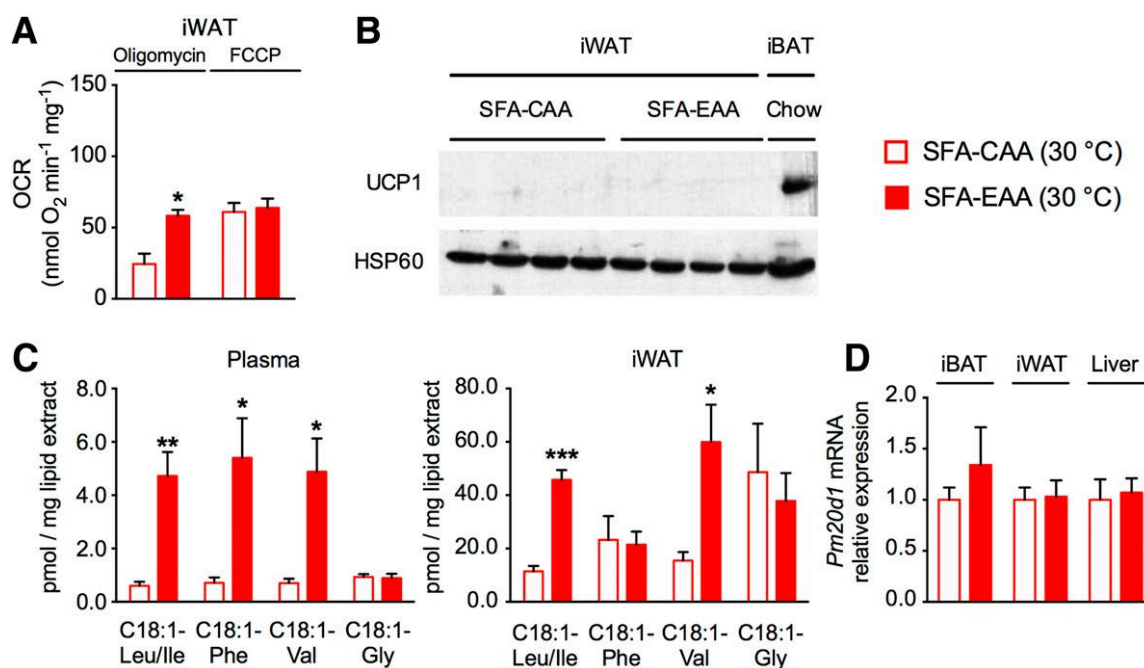


**Figure 5**—The SFA-EAA diet promotes uncoupled respiration in iWAT without browning stimulation. **A**: Uncoupled (i.e., with oligomycin) and maximal (i.e., with FCCP) OCRs in iWAT mitochondria; respiration was normalized to mitochondrial protein amount ( $n = 5$  mice per group). **B**: Western blot analysis of UCP1 and HSP60 protein levels in adipose tissues ( $n = 4$  mice per group). One experiment representative of three reproducible ones is shown. iBAT of mice fed with the chow diet at room temperature was used as the control. **C**: Thermogenic *N*-acyl amino acids in plasma (left) and iWAT (right) ( $n = 4$ –5 mice per group). **D**: Relative mRNA levels of the *Pm20d1* gene in different tissues ( $n = 5$  mice per group). **A–D**: Mice were fed with the SFA-CAA and SFA-EAA diet for 6 weeks at thermoneutrality. All data are presented as mean  $\pm$  SEM. \* $P < 0.05$ , \*\* $P < 0.01$ , and \*\*\* $P < 0.001$  vs. SFA-CAA diet.

This result suggested that the SFA-EAA diet could promote specific UCP1-independent thermogenic processes by which body temperature is increased (Fig. 5A and B and Supplementary Fig. 9A). Although not directly investigated at a biochemical level, gene expression analysis suggested that futile cycling, including the glycerol phosphate shuttle, calcium release and reuptake, and creatine-driven substrate cycling (44), remained unchanged after consuming the SFA-EAA diet (Supplementary Fig. 10A–C), as well as mitochondrial biogenesis and function in skeletal muscle (Supplementary Fig. 10D–F). Because *N*-acyl amino acids stimulate uncoupled mitochondrial respiration in white adipocytes, independently of UCP1 (34), we also measured the levels of *N*-lipidated amino acids in both the plasma and iWAT of SFA-CAA- and SFA-EAA-fed mice housed at 30°C. The circulating and adipose levels of specific C18:1-amino acids were higher in SFA-EAA than in SFA-CAA mice (Fig. 5C). The *N*-acyl amino acids were undetectable in the interscapular adipose tissue (iBAT) of mice fed with both diets. The mRNA levels of *Pm20d1* (peptidase M20 domain-containing 1), the enzyme secreted by thermogenic adipose cells that regulates *N*-acyl amino acids, were unaltered in iWAT, iBAT, and liver of SFA-CAA- and SFA-EAA-fed mice (Fig. 5D).

#### Effects on Brown Adipocytes

Next, by using infrared thermography, we found that after 6 weeks of dietary treatment, iBAT temperature was

higher in mice fed with the SFA-EAA diet compared with those fed with the SFA-CAA diet (Fig. 6A). Interestingly, already at day 5 of treatment, the SFA-EAA diet promoted an uncoupled respiration and UCP1 protein expression in iBAT mitochondria compared with the control diet (Fig. 6B and C). These effects were also maintained after 6 weeks of treatment (Fig. 6D and E). Although thermogenic genes type 2 iodothyronine deiodinase (*Dio2*) and *Prdm16* were unaffected, we found an increased expression of nuclear-encoded respiratory complex genes and of mtDNA amount, in addition to *Ucp1* and *eNOS*, in iBAT of mice fed with the SFA-EAA diet (Supplementary Fig. 11A–C). Moreover, the expression level of the lipolysis-related gene adipose triglyceride lipase (*Atgl*) was higher in iBAT of mice fed with the SFA-EAA diet than with the SFA-CAA diet (Supplementary Fig. 11D). This was accompanied by a greater preponderance of small lipid droplets (Supplementary Fig. 11E) and a higher level of NEFAs in iBAT of SFA-EAA mice (Supplementary Fig. 11F). These results suggested that fatty acid oxidation was increased in iBAT; accordingly, RER was decreased (Fig. 3C), while carnitine palmitoyltransferase 1 (CPT1) activity was increased in iBAT of mice consuming the SFA-EAA diet (Supplementary Fig. 11G).

The mitochondrial respiratory electron transport chain cytochrome c oxidase subunit IV (COX IV) and cytochrome c (Cyt c) protein levels were higher in iBAT of SFA-EAA than SFA-CAA mice (Fig. 6E), suggesting increased mitochondrial

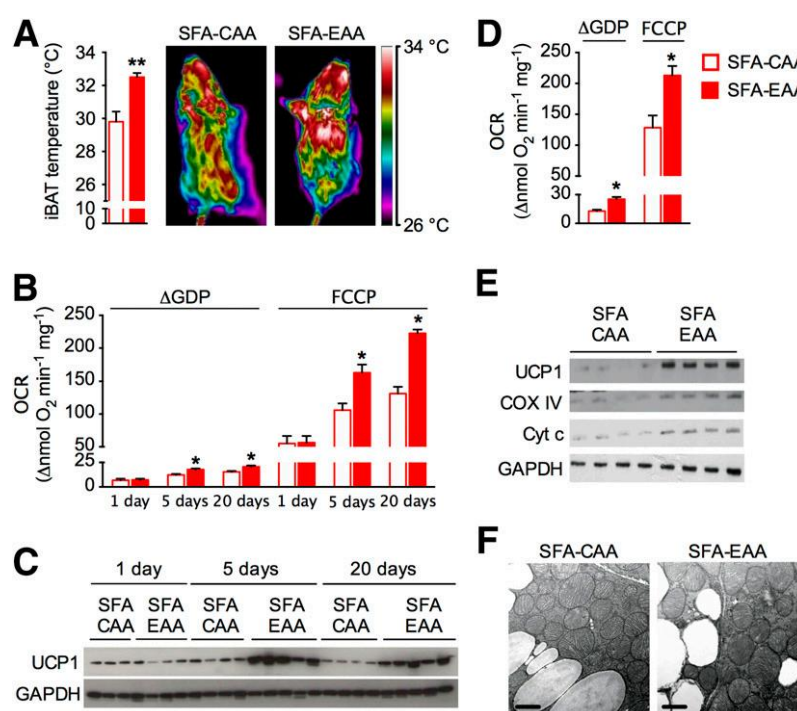


**Figure 6**—SFA-EAA diet increases the thermogenic function of iBAT. **A**: iBAT temperature was measured with a thermographic FLIR camera in mice fed with the SFA-CAA and SFA-EAA diet for 6 weeks at room temperature ( $n = 5$  mice per group). **B**: Uncoupled (i.e.,  $\Delta$ GDP, UCP1-dependent respiration calculated as the amount of ADP-independent respiration that was inhibited by GDP) and maximal (FCCP) OCRs in iBAT mitochondria; respiration was normalized to mitochondrial protein amount ( $n = 5$  mice per group). **C**: Western blot analysis of UCP1 and GAPDH protein levels in iBAT. One experiment representative of three reproducible ones is shown ( $n = 3$ –5 mice per group). Mice in **B** and **C** were fed with the SFA-CAA and SFA-EAA diet for 1, 5, or 20 days at room temperature. **D**: Uncoupled ( $\Delta$ GDP) and maximal (FCCP) OCR in iBAT mitochondria ( $n = 6$  mice per group). **E**: Western blot analysis of UCP1, cytochrome c oxidase subunit IV (COX IV), cytochrome c (Cyt c), and GAPDH protein levels in iBAT. One experiment representative of three reproducible ones is shown ( $n = 4$  mice per group). **F**: Electron microscopy analysis of iBAT. Scale bar, 0.5  $\mu$ m ( $n = 2$  mice per group). Mice in **D**–**F** were fed with the SFA-CAA and SFA-EAA diet for 6 weeks at room temperature. All data are presented as mean  $\pm$  SEM. \* $P < 0.05$  and \*\* $P < 0.01$  vs. SFA-CAA diet.

biogenesis. In accordance, the density of the mitochondrial cristae was augmented (SFA-EAA diet:  $23.64 \pm 0.48 \mu\text{m}^{-2}$  vs. SFA-CAA diet:  $17.83 \pm 0.43 \mu\text{m}^{-2}$ ;  $n = 600$  mitochondria for each sample,  $P < 0.0001$ ), although mitochondrial density was similar in both diets (SFA-EAA: 8.9 over  $10 \mu\text{m}^2$  vs. SFA-CAA: 8.1 over  $10 \mu\text{m}^2$ , NS) and mitochondrial area was reduced (SFA-EAA diet:  $0.58 \pm 0.017 \mu\text{m}^2$  vs. SFA diet-CAA:  $0.71 \pm 0.018 \mu\text{m}^2$ ,  $P < 0.0001$ ) by the SFA-EAA diet (Fig. 6F). Congruently, iBAT was activated in obese *ob/ob* mice (Supplementary Fig. 9B–D). Overall, our findings suggest that the SFA-EAA diet was able to activate an iBAT thermogenic program, in which utilization (i.e., oxidation) of fatty acids is increased.

#### Effects on Brown Adipocyte Activators

Thus, we investigated how the SFA-EAA diet activates the thermogenic program in iBAT. Fibroblast growth factor 21 (FGF21), which promotes sympathetic nerve activity in brown fat, browning of iWAT, and energy expenditure in diet-induced obese mice (45), was lower in the plasma of the SFA-EAA-fed mice, accordingly to reduced *Fgf21* gene expression in liver and adipose. These observations may be of interest, because elevated circulating FGF21 is noted in

impaired glucose tolerance and type 2 diabetes and correlates with muscle and hepatic insulin resistance (46) and not only with increased thermogenesis and metabolic homeostasis improvement (45) (Supplementary Fig. 12A and B). Analogously, long-chain acylcarnitines, synthesized in the liver in response to cold exposure or treatment with  $\beta_3$ -adrenergic receptor agonists and providing fuel for iBAT thermogenesis (47), were unchanged in the plasma of mice fed with either diet, similarly to the expression of genes involved in their metabolism in the liver, iBAT (except for *CrAT*), and muscle (Supplementary Fig. 12C and D).

Also, there was no apparent difference of NE turnover—a direct neurochemical measure of sympathetic nervous system (SNS) activity and a proxy of sympathetic innervation (48)—in iBAT of SFA-EAA mice versus SFA-CAA mice—as well as of tyrosine hydroxylase and  $\beta_3$ -adrenoceptor expression, markers of noradrenergic innervation (Fig. 7A and B). Given that sympathetic denervation of iBAT—both surgical and chemical—has limitations, especially when used to study the involvement of the SNS in systemic effects of chronic treatments, we chose to develop an in vitro system to confirm that the SFA-EAA diet may

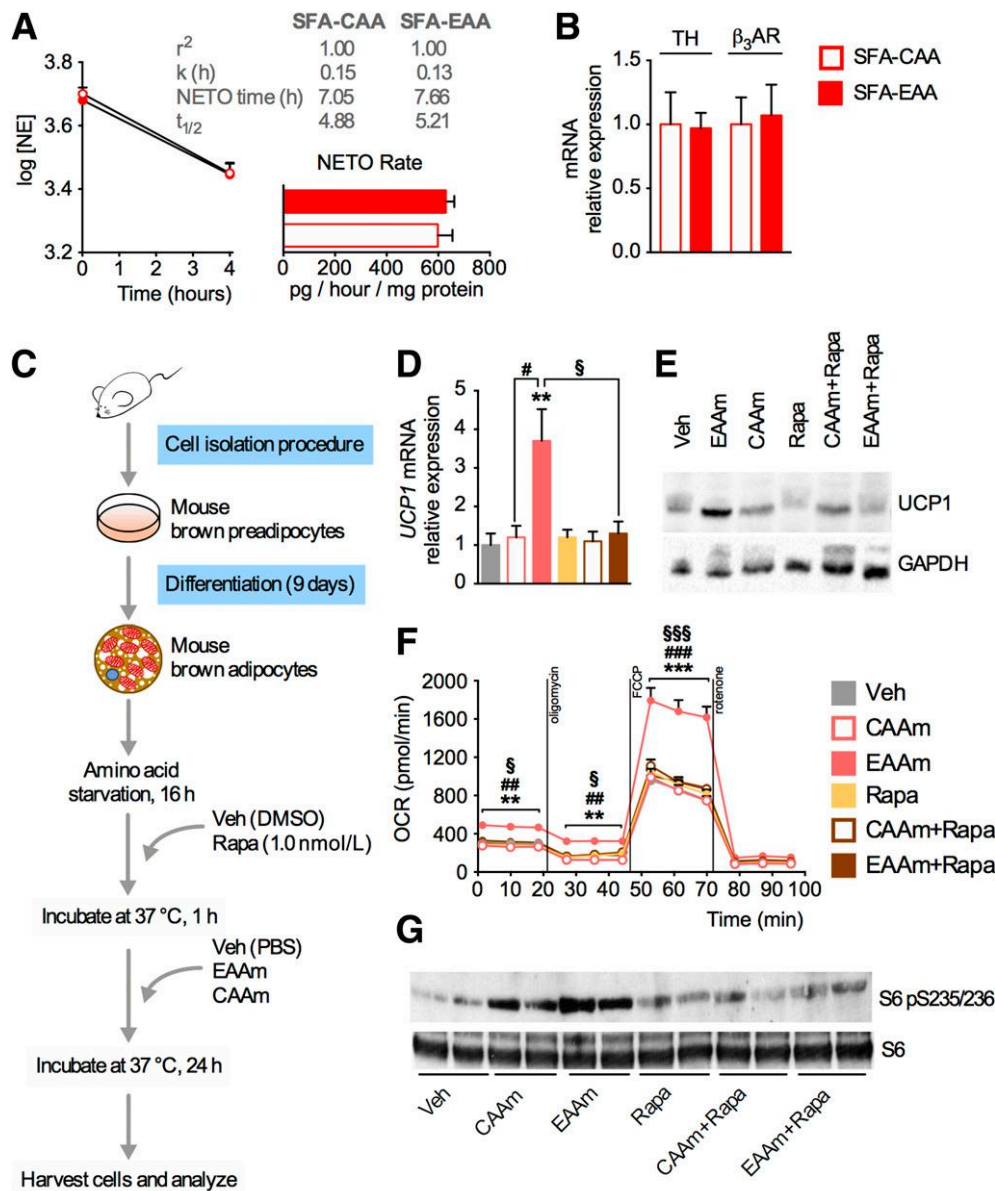


**Figure 7**—The SFA-EAA diet activates brown adipocytes. **A**: NE turnover (NETO) in iBAT of mice fed with the SFA-CAA and SFA-EAA diet for 6 weeks at room temperature. NETO was assessed by NE synthesis inhibition with  $\alpha$ -methyl-*p*-tyrosine ( $n = 5$  mice per group). **B**: Relative mRNA levels of noradrenergic innervation markers in iBAT of mice fed with the SFA-CAA and SFA-EAA diet for 6 weeks. **C**: Scheme of the in vitro experiment in primary brown adipocytes isolated from mice fed with the chow diet. After 16-h incubation in amino acid-free medium, brown adipocytes were pretreated with rapamycin (Rapa, 1.0 nmol/L) or vehicle (Veh; DMSO) for 1 h. Then, the cells were incubated with Veh (PBS) or CAA mixture (CAAM) or EAA mixture (EAAM), specifically reproducing the iBAT aminograms resulting from consumption of either the SFA-CAA or SFA-EAA diets, respectively, as reported in Supplementary Table 4 ( $n = 3$  experiments performed in triplicate). **D**: *Ucp1* mRNA levels in differentiated brown adipocytes, treated as in **C**. Western blot analysis of UCP1 and GAPDH (**E**), and (Ser 235/236) phosphorylated (p) S6 and S6 (**G**) protein levels in differentiated brown adipocytes, treated as in **C**. One immunoblot experiment representative of three reproducible ones is shown. **F**: OCRs of differentiated brown adipocytes, treated as in **C**. OCR was measured with the Seahorse XF24 Extracellular Flux Analyzer ( $n = 3$  readings in quadruplicate per group). All data are presented as mean  $\pm$  SEM.  $**P < 0.01$  and  $***P < 0.001$  vs. Veh;  $\#P < 0.05$ ,  $\#\#P < 0.01$ , and  $\#\#\#P < 0.001$  vs. CAAM;  $\$P < 0.05$  and  $\$\$\$P < 0.001$  vs. EAAM + Rapa. TH, tyrosine hydroxylase;  $\beta_3$ AR,  $\beta_3$ -adrenergic receptor.

act directly on brown adipocytes independently of SNS. In particular, we exposed primary brown adipocytes differentiated in culture to one of two different amino acid combinations, precisely reproducing the iBAT aminograms resulting from consumption of either the SFA-CAA or

SFA-EAA diets (Fig. 7C and Supplementary Table 4). Notably, the EAA mixture increased both UCP1 mRNA and protein levels and, accordingly, the uncoupled respiration when compared with vehicle-treated cells (Fig. 7D–F). Conversely, the CAA mixture failed to promote



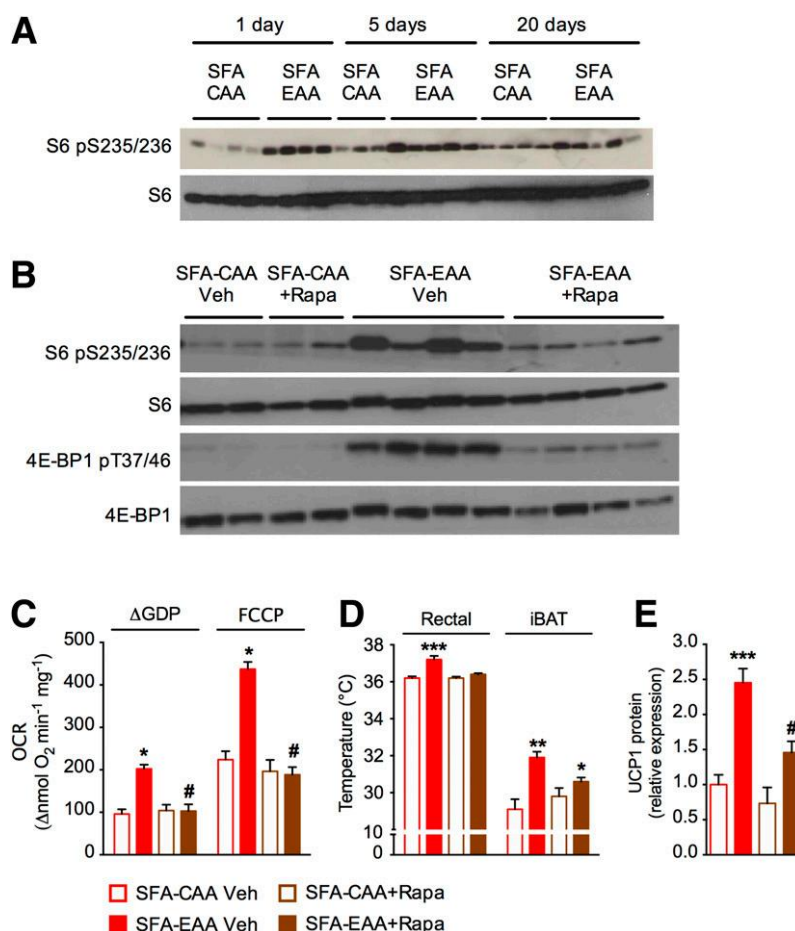


**Figure 8**—mTORC1 signaling contributes to iBAT thermogenesis induced by the SFA-EAA diet. **A**: Western blot analysis of (Ser 235/236) phosphorylated (p) S6 and S6 protein levels in iBAT of mice fed with the SFA-CAA and SFA-EAA diet for different time intervals at room temperature. One immunoblot experiment representative of three reproducible ones is shown ( $n = 3$ –5 mice per group). **B**: Western blot analysis of the mTORC1 pathway in iBAT of mice fed with the SFA-CAA and SFA-EAA diet, with vehicle (Veh) or rapamycin (Rapa) ( $n = 4$  mice per group). **C**: UCP1-dependent ( $\Delta$ GDP) and maximal (FCCP) OCRs in iBAT mitochondria. OCR was normalized to mitochondrial protein amount ( $n = 5$  mice per group). **D**: Rectal and thermographic measurement of iBAT temperature ( $n = 5$  mice per group). **E**: Western blot analysis of UCP1 protein levels in iBAT. Mice in **B**–**E** were fed with the SFA-CAA or SFA-EAA diet for 6 weeks at room temperature, with or without rapamycin (i.p. 2.5 mg/kg body wt) delivered in 200  $\mu$ L, 5 days per week for 6 weeks, starting with diets ( $n = 5$ –6 mice per group). All data are presented as mean  $\pm$  SEM. \* $P < 0.05$ , \*\* $P < 0.01$ , and \*\*\* $P < 0.001$  vs. SFA-CAA diet; # $P < 0.05$  vs. SFA-EAA diet. 4E-BP1, eukaryotic initiation factor 4E-binding protein 1.

either UCP1 expression or  $VO_2$ . Together, these findings seem to suggest that the effects of the SFA-EAA diet on iBAT depend mainly on a brown adipocyte autonomous process.

### Effects on Thermogenic Signaling

We next aimed to investigate the molecular mechanism of iBAT activation by studying the role of the mTOR signaling pathway activated by amino acids and required for brown fat recruitment and metabolic adaptation to cold exposure (29,30). The exposure of primary brown adipocytes in culture to the EAA mixture markedly promoted mTOR activation, as shown by the phosphorylation of the mTORC1-downstream target ribosomal protein S6 (S6) (Fig. 7G). Despite a partial efficacy of the CAA mixture in the mTOR activation, however, this effect was not associated with stimulation of the

UCP1-dependent thermogenic program. In turn, rapamycin, the macrolide antibiotic that selectively inhibits mTORC1, fully antagonized the stimulatory effect of the EAA mixture on the expression of UCP1 and markers of mitochondrial biogenesis (Fig. 7E). These results were confirmed in vivo in the C57BL6/N and *ob/ob* mice (Fig. 8 and Supplementary Fig. 13). Already at day 1 of treatment, the SFA-EAA diet consistently increased S6 phosphorylation in iBAT (Fig. 8A). Our data showed that this effect was iBAT-specific, without any phosphorylation of S6 and 4E-BP1 (eukaryotic translation initiation factor 4E-binding protein 1) in iWAT and gastrocnemius muscle after 6 weeks of feeding with the SFA-EAA diet (Supplementary Fig. 13B). The systemic administration of rapamycin entirely blocked  $VO_2$  and S6 and 4E-BP1 phosphorylation in iBAT of the SFA-EAA-fed mice (Fig. 8B and C). These effects were



accompanied by a blockade of action of this diet on core and iBAT temperature, UCP1 expression in brown fat, as well as on body weight and adiposity, without affecting food intake (Fig. 8D and E and Supplementary Fig. 13C and D).

## DISCUSSION

Collectively, our data reveal that customized diets, in which a precise formula of EAAs substitutes for protein content—without changing calorie content and macronutrient percentage—exert preventive and therapeutic anti-obesity effects, with amelioration of body adiposity, insulin resistance, and fatty liver, beyond promoting a longer and healthier life span. The beneficial effects of either the SFA-EAA or HFD-EAA diet on longevity and metabolic homeostasis can be secondary to reduced adiposity, even if the ability of our particular amino acid combination to play a primary action cannot be excluded.

Although with the EAA-substituted diets certain EAAs (i.e., histidine, isoleucine, leucine, lysine, threonine, and valine) were consumed in a higher amount, while others (i.e., methionine, phenylalanine, and tyrosine) in lower amounts than those recommended for mice by the U.S. National Research Council (Supplementary Table 10), the circulating levels of EAAs and NEAAs do not seem to exceed tolerable upper and lower levels for individual amino acids. Although few studies report the adverse effects of chronic intake of specific amino acid supplements and there is no adequate dose–response data from human or animal studies to base accepted limits, our results with life-long consumption of markedly changed amino acid combinations are conversely reassuring. They show that diets with very restricted—yet not wholly lacking—amounts of NEAAs (i.e., the SFA-EAA and HFD-EAA diets) are healthy and do not alter animal growth. Traditionally viewed as amino acids that can be synthesized *de novo* in adequate amounts by the animal organism to meet the requirements for growth and maintenance, the nutritionally NEAAs are currently considered, in a correct way, necessary for multiple roles in physiology. NEAAs participate in gene expression, cell signaling pathways, and antioxidative responses in addition to regulating neurotransmission and immunity; thus, their nonessentiality has been questioned.

Reduction of food intake and gut energy absorption do not appear to play relevant roles in the healthy effects of our substituted diets. This conclusion seems to be confirmed by the absence in mice fed with the SFA-EAA or HFD-EAA diets of the physiological adjustments that animals usually exhibit to maintain energy balance when subjected to a decrease in resource availability; for example, as increased exploratory activities and intestinal energy absorption (49) or reduced basal metabolic rate and NST. The NST is indeed increased in SFA-EAA- and HFD-EAA-fed mice. While browning of iWAT is not induced, a UCP1's independent uncoupling of respiration is evident

in iWAT of SFA-EAA-fed mice and potentially may promote thermogenesis. Despite the possibility that the observed increase of lipidated amino acid levels in iWAT could be responsible for this higher uncoupled respiration, their relative contribution to the overall phenotype of SFA-EAA (and also of HFD-EAA) mice remains to be addressed. Most significantly, the SFA-EAA and HFD-EAA diets promote marked iBAT activation in both normal weight and obese mice, irrespective of the environmental temperature. FGF21, acylcarnitines, NE, and thyroid hormones, well-known activators of brown fat (45,47), are not responsible for the beneficial effects of the SFA-EAA diet. Similarly, other thermogenic mechanisms, including the UCP1-independent futile cycling and muscle mitochondrial biogenesis, are not promoted by the SFA-EAA diet.

Conversely, iBAT thermogenesis could be directly activated by the specific combination of amino acids in this tissue. The EAA mixture, unlike the CAA mixture, which were designed on the profiles of amino acids identified in iBAT of SFA-EAA- and SFA-CAA-fed mice (iBAT aminograms), respectively, promotes a thermogenic program in cultured brown adipocytes through activation of mTORC1 signaling. Notably, the iBAT aminograms differ between mice fed with the two dietary regimens: arginine, isoleucine, leucine, proline, threonine, and valine are statistically higher in SFA-EAA- than in SFA-CAA-fed mice, while, on the contrary, glycine, lysine, and serine are lower. From the literature, isoleucine, leucine, and valine (namely, the branched-chain amino acids) supplementation ameliorates some metabolic dysfunction caused by obesity or diabetes, without impairing glucose metabolism, in some studies (50) but not in others (51,52). Arginine, as a substrate of nitric oxide synthase, produces nitric oxide (NO) for signaling purposes, including mitochondrial biogenesis and thermogenic program in iBAT (39). Increasing evidence has shown that dietary supplementation of arginine can effectively improve BAT thermogenesis via the mTOR signaling pathway (53), with reduced obesity and diabetes, in addition to improved obesity-linked dyslipidemia and high blood pressure in mammals, including humans (54). Similarly, proline supplementation improves NO bioavailability and counteracts the blood pressure (55). By contrast, the SFA-EAA diet reduced the NEAA glycine levels in iBAT compared with the SFA-CAA diet, and accordingly, the glycine precursor threonine was increased. Of note, neuronal glycine has been found to inhibit sympathetic activation of BAT (56), and although circulating glycine is low in obese subjects and its supplementation was proposed as a treatment of obesity (57), no clear role has been found in brown fat. Also for serine, which was similarly reduced in SFA-EAA mice, further studies are needed to confirm and extend our findings.

Additionally, we observed some interesting differences in microbiota composition. There was an enrichment of *Allobaculum* and *Sutterella* in the gut of mice fed with the SFA-EAA diet compared with the SFA and SFA-CAA diets, which might play some role in light of the inverse correlation we observed with body weight and insulin

resistance, in agreement with previous observations (58). Several studies have demonstrated that the HFD reduces the relative abundance of both taxa in the gut of mice, while multiple dietary interventions, such as prebiotics, probiotics, and berberine, which ameliorate insulin resistance and adipose inflammation, promote the relative abundance of both *Allobaculum* and *Sutterella* (59,60). Again, mounting evidence suggests that gut microbiota can stimulate brown fat thermogenesis in mice (37,58). Further studies are therefore warranted to establish metabolic links between gut bacteria, such as *Allobaculum* and *Sutterella*, and the iBAT activation by our diets.

Similarly, additional work is necessary to understand whether the longevity effects of SFA-EAA are simply due to the reduced adiposity or to a direct action of our peculiar amino acid combination. Remarkably, reducing the NEAA concentration has been found to promote replicative life span extension in yeast (61); as in turn, increasing EAA concentration prolongs the life span not only in yeast but also in *Caenorhabditis elegans* and, most importantly, in mammals (14,62,63). The increased chronological life span extension of yeast promoted by EAA supplementation was found to be accompanied by lower oxidative damage and notably by the activation, not inhibition as often reported with other life span prolonging methods, of the TOR signaling pathway (61). Yang et al. (19) have moreover reported that an amino acid formula similar to the amino acid combination in our EAA-substituted diets slowed the age-related changes of gut microbiota, without affecting body weight, suggesting that the dietary supplementation might promote healthy aging independently of its effects on adiposity.

Because our EAA-substituted diets are deficient of some EAAs compared with controls, one could claim that detection of amino acid unbalance or, alternately, a restriction of specific amino acids may be relevant intermediaries to the beneficial effects of both SFA-EAA and HFD-EAA diets. These possibilities were proposed to interpret previous findings. For example, mice fed with diets lacking the single EAA tryptophan had increased resistance to surgical stress as well as improved longevity, metabolic fitness, and stress resistance (64). However, detection of dietary amino acid imbalance seems improbable in our case because there is no apparent change of the GCN2 activity, the critical regulator of cellular responses under amino acid deficiency or imbalance, in both hypothalamus and liver of mice under the different dietary regimens. Moreover, previous studies have shown that diets deficient in EAAs can influence food intake and increase FGF21 levels (65). Consuming the SFA-EAA diet, conversely, does not change feeding and decreases circulating and hepatic FGF21 levels. Also, feeding rodents survival-promoting methionine-restricted diets comprising purified amino acids as the sole source of nitrogenous content causes some of the phenotypes described here, including protection from weight gain (mostly in adiposity), improved glucose homeostasis, increased energy expenditure, and activation of iBAT (66).

However, the abundance of cysteine in the SFA-EAA and HFD-EAA diets rules out methionine-restriction as the key mechanism behind the present findings.

In summary, the current study indicates that specific manipulation of dietary amino acids prevents and reverses obesity in mice through multiple modes to stimulate thermogenesis. Reasonably, taken separately from each other, these multiple modes would be unable to explain the overall observed results. If extended to humans, such dietary manipulation could potentially have a positive impact on metabolic health favoring the prevention and treatment of obesity and type 2 diabetes regardless of calorie consumption.

**Acknowledgments.** The authors thank M. Rossato (Department of Medicine, University of Padua, Padua, Italy) for experiments with the FLIR camera, Mariaelvina Sala and Daniela Braida (Department of Medical Biotechnology and Translational Medicine, University of Milan, Milan, Italy) for behavioral experiments, Annapaola Andolfo and Cinzia Magagnotti (Protein Microsequencing Facility, San Raffaele Scientific Institute, Milan, Italy) for mass spectrometry analysis, and Alessandra Micheletti (Department of Environmental Sciences and Politics, University of Milan, Milan, Italy) and Marika Vezzoli (Department of Molecular and Translational Medicine, Brescia University, Brescia, Italy) for statistical analysis.

**Funding.** This work was supported by Fondazione Umberto Veronesi to C.R., University of Milan to F.R. (Research Fellowship grant 1280/2016), Professional Dietetics (Milan, Italy) to E.N. (support to laboratory), Cariplo Foundation to E.N. and to A.V. (grant 2016-1006), and Louis-Jeantet Foundation grant to R.C.

**Duality of Interest.** No potential conflicts of interest relevant to this article were reported.

**Author Contributions.** C.R. and M.R. designed and performed molecular biology, metabolic,  $VO_2$ , and animal experiments. C.R., M.R., and E.N. wrote the manuscript with suggestions from all authors, all of whom read and approved the final version. F.R. and L.Ted. performed in vitro experiments and quantitative RT-PCR analysis. P.C., C.M.G., D.L., and R.P.C. designed and performed experiments in animals. V.G., L.Ten., and C.L. designed and analyzed experiments on metabolites. F.P., A.C., and V.D.M. designed, performed, and analyzed liquid chromatography-mass spectroscopy experiments for *N*-acyl-amino acid and acylcarnitine measurements. E.M. synthesized *N*-acyl-amino acids. R.M.I., F.Bo., and R.C. designed, performed, and analyzed indirect calorimetry experiments. A.P. and I.D. performed experiments at thermoneutrality. L.P. designed, performed, and analyzed behavioral experiments. I.S. and S.Ci. designed, performed, and analyzed electron microscopy and histological experiments. L.R., M.S., and K.T. performed microbiota analysis. F.Bi., M.O.C., G.C., R.C., S.Co., and A.V. assisted with experimental design and coedited the manuscript. E.N. conceived the study, designed experiments, and provided advice. E.N. is the guarantor of this work and, as such, had full access to all the data in the study and takes responsibility for the integrity of the data and the accuracy of the data analysis.

## References

1. Koska J, Ozias MK, Deer J, et al. A human model of dietary saturated fatty acid induced insulin resistance. *Metabolism* 2016;65:1621–1628
2. Vasilopoulou D, Markey O, Kliem KE, et al. Reformulation initiative for partial replacement of saturated with unsaturated fats in dairy foods attenuates the increase in LDL cholesterol and improves flow-mediated dilatation compared with conventional dairy: the randomized, controlled REplacement of SaturatEd fat in dairy on Total cholesterol (RESET) study. *Am J Clin Nutr* 2020;111:739–748
3. Scherer PE. The many secret lives of adipocytes: implications for diabetes. *Diabetologia* 2019;62:223–232

4. Hall KD, Ayuketah A, Brychta R, et al. Ultra-processed diets cause excess calorie intake and weight gain: an inpatient randomized controlled trial of ad libitum food intake. *Cell Metab* 2019;30:67–77.e3
5. Gardner CD, Kiazand A, Alhassan S, et al. Comparison of the Atkins, Zone, Ornish, and LEARN diets for change in weight and related risk factors among overweight premenopausal women: the A TO Z Weight Loss Study: a randomized trial. *JAMA* 2007;297:969–977
6. Lagiou P, Sandin S, Lof M, Trichopoulos D, Adami HO, Weiderpass E. Low carbohydrate-high protein diet and incidence of cardiovascular diseases in Swedish women: prospective cohort study. *BMJ* 2012;344:e4026
7. Huang X, Hancock DP, Gosby AK, et al. Effects of dietary protein to carbohydrate balance on energy intake, fat storage, and heat production in mice. *Obesity (Silver Spring)* 2013;21:85–92
8. Fontana L, Cummings NE, Arriola Apelo SI, et al. Decreased consumption of branched-chain amino acids improves metabolic health. *Cell Rep* 2016;16:520–530
9. Anthony TG, Morrison CD, Gettys TW. Remodeling of lipid metabolism by dietary restriction of essential amino acids. *Diabetes* 2013;62:2635–2644
10. Binder E, Bermúdez-Silva FJ, André C, et al. Leucine supplementation protects from insulin resistance by regulating adiposity levels. *PLoS One* 2013;8:e74705
11. Serra F, LeFeuvre RA, Slater D, Palou A, Rothwell NJ. Thermogenic actions of tryptophan in the rat are mediated independently of 5-HT. *Brain Res* 1992;578:327–334
12. Nairizi A, She P, Vary TC, Lynch CJ. Leucine supplementation of drinking water does not alter susceptibility to diet-induced obesity in mice. *J Nutr* 2009;139:715–719
13. Bifari F, Nisoli E. Branched-chain amino acids differently modulate catabolic and anabolic states in mammals: a pharmacological point of view. *Br J Pharmacol* 2017;174:1366–1377
14. D'Antona G, Ragni M, Cardile A, et al. Branched-chain amino acid supplementation promotes survival and supports cardiac and skeletal muscle mitochondrial biogenesis in middle-aged mice. *Cell Metab* 2010;12:362–372
15. D'Antona G, Tedesco L, Ruocco C, et al. A peculiar formula of essential amino acids prevents rosvastatin myopathy in mice. *Antioxid Redox Signal* 2016;25:595–608
16. Bifari F, Dolci S, Bottani E, et al. Complete neural stem cell (NSC) neuronal differentiation requires a branched chain amino acids-induced persistent metabolic shift towards energy metabolism. *Pharmacol Res* 2020;158:104863
17. Brunetti D, Bottani E, Segala A, et al. Targeting multiple mitochondrial processes by a metabolic modulator prevents sarcopenia and cognitive decline in SAMP8 mice. *Front Pharmacol* 2020;11:1171
18. Buondonno I, Sassi F, Carignano G, et al. From mitochondria to healthy aging: the role of branched-chain amino acids treatment: MATeR a randomized study. *Clin Nutr* 2020;39:2080–2091
19. Yang Z, Huang S, Zou D, et al. Metabolic shifts and structural changes in the gut microbiota upon branched-chain amino acid supplementation in middle-aged mice. *Amino Acids* 2016;48:2731–2745
20. Ridaura VK, Faith JJ, Rey FE, et al. Gut microbiota from twins discordant for obesity modulate metabolism in mice. *Science* 2013;341:1241214
21. Sharon G, Garg N, Debelius J, Knight R, Dorrestein PC, Mazmanian SK. Specialized metabolites from the microbiome in health and disease. *Cell Metab* 2014;20:719–730
22. Cox LM, Yamanishi S, Sohn J, et al. Altering the intestinal microbiota during a critical developmental window has lasting metabolic consequences. *Cell* 2014;158:705–721
23. Li B, Li L, Li M, et al. Microbiota depletion impairs thermogenesis of brown adipose tissue and browning of white adipose tissue. *Cell Rep* 2019;26:2720–2737.e5
24. Shabalina IG, Petrovic N, de Jong JMA, Kalinovich AV, Cannon B, Nedergaard J. UCP1 in brite/beige adipose tissue mitochondria is functionally thermogenic. *Cell Rep* 2013;5:1196–1203
25. Cohen P, Levy JD, Zhang Y, et al. Ablation of PRDM16 and beige adipose causes metabolic dysfunction and a subcutaneous to visceral fat switch. *Cell* 2014;156:304–316
26. Lowell BB, S-Susulic V, Hamann A, et al. Development of obesity in transgenic mice after genetic ablation of brown adipose tissue. *Nature* 1993;366:740–742
27. Feldmann HM, Golozoubova V, Cannon B, Nedergaard J. UCP1 ablation induces obesity and abolishes diet-induced thermogenesis in mice exempt from thermal stress by living at thermoneutrality. *Cell Metab* 2009;9:203–209
28. Seale P, Conroe HM, Estall J, et al. Prdm16 determines the thermogenic program of subcutaneous white adipose tissue in mice. *J Clin Invest* 2011;121:96–105
29. Liu D, Bordicchia M, Zhang C, et al. Activation of mTORC1 is essential for  $\beta$ -adrenergic stimulation of adipose browning. *J Clin Invest* 2016;126:1704–1716
30. Labbé SM, Mouchiroud M, Caron A, et al. mTORC1 is required for brown adipose tissue recruitment and metabolic adaptation to cold. *Sci Rep* 2016;6:37223
31. Brown LJ, Koza RA, Everett C, et al. Normal thyroid thermogenesis but reduced viability and adiposity in mice lacking the mitochondrial glycerol phosphate dehydrogenase. *J Biol Chem* 2002;277:32892–32898
32. Ikeda K, Kang Q, Yoneshiro T, et al. UCP1-independent signaling involving SERCA2b-mediated calcium cycling regulates beige fat thermogenesis and systemic glucose homeostasis. *Nat Med* 2017;23:1454–1465
33. Kazak L, Chouchani ET, Lu GZ, et al. Genetic depletion of adipocyte creatine metabolism inhibits diet-induced thermogenesis and drives obesity. *Cell Metab* 2017;26:660–671.e3
34. Long JZ, Svensson KJ, Bateman LA, et al. The secreted enzyme PM20D1 regulates lipidated amino acid uncouplers of mitochondria. *Cell* 2016;166:424–435
35. Fontaine DA, Davis DB. Attention to background strain is essential for metabolic research: C57BL/6 and the International Knockout Mouse Consortium. *Diabetes* 2016;65:25–33
36. Ramadori G, Fujikawa T, Fukuda M, et al. SIRT1 deacetylase in POMC neurons is required for homeostatic defenses against diet-induced obesity. *Cell Metab* 2010;12:78–87
37. Chevalier C, Stojanović O, Colin DJ, et al. Gut microbiota orchestrates energy homeostasis during cold. *Cell* 2015;163:1360–1374
38. Lister RG. The use of a plus-maze to measure anxiety in the mouse. *Psychopharmacology (Berl)* 1987;92:180–185
39. Nisoli E, Clementi E, Paolucci C, et al. Mitochondrial biogenesis in mammals: the role of endogenous nitric oxide. *Science* 2003;299:896–899
40. Bieber LL, Abraham T, Helmrath T. A rapid spectrophotometric assay for carnitine palmitoyltransferase. *Anal Biochem* 1972;50:509–518
41. Gordon CJ. The mouse thermoregulatory system: its impact on translating biomedical data to humans. *Physiol Behav* 2017;179:55–66
42. Kanazawa I, Yamaguchi T, Sugimoto T. Serum insulin-like growth factor-I is negatively associated with serum adiponectin in type 2 diabetes mellitus. *Growth Horm IGF Res* 2011;21:268–271
43. Dever TE, Feng L, Wek RC, Cigan AM, Donahue TF, Hinnebusch AG. Phosphorylation of initiation factor 2  $\alpha$  by protein kinase GCN2 mediates gene-specific translational control of GCN4 in yeast. *Cell* 1992;68:585–596
44. Chouchani ET, Kazak L, Spiegelman BM. New advances in adaptive thermogenesis: UCP1 and beyond. *Cell Metab* 2019;29:27–37
45. Kliewer SA, Mangelsdorf DJ. A dozen years of discovery: insights into the physiology and pharmacology of FGF21. *Cell Metab* 2019;29:246–253
46. Chavez AO, Molina-Carrion M, Abdul-Ghani MA, Folli F, Defronzo RA, Tripathy D. Circulating fibroblast growth factor-21 is elevated in impaired glucose tolerance and type 2 diabetes and correlates with muscle and hepatic insulin resistance. *Diabetes Care* 2009;32:1542–1546

47. Simcox J, Geoghegan G, Maschek JA, et al. Global analysis of plasma lipids identifies liver-derived acylcarnitines as a fuel source for brown fat thermogenesis. *Cell Metab* 2017;26:509–522.e6
48. Vaughan CH, Zarebidaki E, Ehlen JC, Bartness TJ. Analysis and measurement of the sympathetic and sensory innervation of white and brown adipose tissue. *Methods Enzymol* 2014;537:199–225
49. Peña-Villalobos I, Casanova-Maldonado I, Lois P, Sabat P, Palma V. Adaptive physiological and morphological adjustments mediated by intestinal stem cells in response to food availability in mice. *Front Physiol* 2019;9:1821
50. Woo S-L, Yang J, Hsu M, et al. Effects of branched-chain amino acids on glucose metabolism in obese, prediabetic men and women: a randomized, crossover study. *Am J Clin Nutr* 2019;109:1569–1577
51. Newgard CB, An J, Bain JR, et al. A branched-chain amino acid-related metabolic signature that differentiates obese and lean humans and contributes to insulin resistance. *Cell Metab* 2009;9:311–326
52. Zhou M, Shao J, Wu CY, et al. Targeting BCAA catabolism to treat obesity-associated insulin resistance. *Diabetes* 2019;68:1730–1746
53. Ma X, Han M, Li D, et al. L-Arginine promotes protein synthesis and cell growth in brown adipocyte precursor cells via the mTOR signal pathway. *Amino Acids* 2017;49:957–964
54. McKnight JR, Satterfield MC, Jobgen WS, et al. Beneficial effects of L-arginine on reducing obesity: potential mechanisms and important implications for human health. *Amino Acids* 2010;39:349–357
55. Leal J, Teixeira-Santos L, Pinho D, et al. L-proline supplementation improves nitric oxide bioavailability and counteracts the blood pressure rise induced by angiotensin II in rats. *Nitric Oxide* 2019;82:1–11
56. Conceição EP, Madden CJ, Morrison SF. Glycinergic inhibition of BAT sympathetic premotor neurons in rostral raphe pallidus. *Am J Physiol Regul Integr Comp Physiol* 2017;312:R919–R926
57. Alves A, Bassot A, Bulteau AL, Pirola L, Morio B. Glycine metabolism and its alterations in obesity and metabolic diseases. *Nutrients* 2019;11:1356
58. Schneeberger M, Everard A, Gómez-Valadés AG, et al. *Akkermansia muciniphila* inversely correlates with the onset of inflammation, altered adipose tissue metabolism and metabolic disorders during obesity in mice. *Sci Rep* 2015;5:16643
59. Everard A, Matamoros S, Geurts L, Delzenne NM, Cani PD. *Saccharomyces boulardii* administration changes gut microbiota and reduces hepatic steatosis, low-grade inflammation, and fat mass in obese and type 2 diabetic *db/db* mice. *MBio* 2014;5:e01011–e01014
60. Zhang X, Zhao Y, Zhang M, et al. Structural changes of gut microbiota during berberine-mediated prevention of obesity and insulin resistance in high-fat diet-fed rats. *PLoS One* 2012;7:e42529
61. Jiang JC, Jaruga E, Repnevskaya MV, Jazwinski SM. An intervention resembling caloric restriction prolongs life span and retards aging in yeast. *FASEB J* 2000;14:2135–2137
62. Aris JP, Alvers AL, Ferraiuolo RA, et al. Autophagy and leucine promote chronological longevity and respiration proficiency during calorie restriction in yeast. *Exp Gerontol* 2013;48:1107–1119
63. Edwards C, Canfield J, Copes N, et al. Mechanisms of amino acid-mediated lifespan extension in *Caenorhabditis elegans*. *BMC Genet* 2015;16:8
64. Gallinetti J, Harputlugil E, Mitchell JR. Amino acid sensing in dietary-restriction-mediated longevity: roles of signal-transducing kinases GCN2 and TOR. *Biochem J* 2013;449:1–10
65. De Sousa-Coelho AL, Marrero PF, Haro D. Activating transcription factor 4-dependent induction of FGF21 during amino acid deprivation. *Biochem J* 2012;443:165–171
66. Wanders D, Burk DH, Cortez CC, et al. UCP1 is an essential mediator of the effects of methionine restriction on energy balance but not insulin sensitivity. *FASEB J* 2015;29:2603–2615